

Effect of symmetry lowering on the dielectric response of BaZrO₃

Joseph W. Bennett, Ilya Grinberg, and Andrew M. Rappe

The Makineni Theoretical Laboratories, Department of Chemistry, University of Pennsylvania, Philadelphia, Pennsylvania 19104-6323

(Received 24 March 2006; published 23 May 2006)

We use first-principles density functional theory calculations to investigate the dielectric response of BaZrO₃ perovskite. A previous study [Akbarzadeh *et al.*, Phys. Rev. B **72**, 205104 (2005)] reported a disagreement between experimental and theoretical low temperature dielectric constant ϵ for the high symmetry BaZrO₃ structure. We show that a fully relaxed 40 atom BaZrO₃ structure exhibits O₆ octahedral tilting, and ϵ that agrees with experiment. The change in ϵ from high-symmetry to low-symmetry structure is due to increased phonon frequencies as well as decreased mode effective charges.

DOI: [10.1103/PhysRevB.73.180102](https://doi.org/10.1103/PhysRevB.73.180102)

PACS number(s): 77.22.-d, 61.66.-f, 63.20.-e

I. INTRODUCTION

Dielectric materials are important for wireless communications technology. These devices require a high dielectric constant, ϵ , and low dielectric loss.¹ Barium zirconate, BaZrO₃ (BZ), is one of the constituent materials in the electroceramic capacitors used in wireless communications. BZ is a classic ABO₃ perovskite dielectric material that is both chemically and mechanically stable.

According to the well-established tolerance factor argument, BZ should have a stable cubic structure. Tolerance factor t is given by

$$t = \frac{R_{A-O}}{R_{B-O}\sqrt{2}}, \quad (1)$$

where R_{A-O} is the sum of A and O ionic radii and R_{B-O} is the sum of B and O ionic radii. Tolerance factor $t < 1$ usually leads to the rotation and expansion of the B-O₆ octahedra. Such octahedral rotations often generate a low temperature anti-ferroelectric (AFE) phase (e.g., PbZrO₃). If $t > 1$, the B-O₆ octahedra are stretched from their preferred B-O bond lengths, promoting B-cation distortions by creating room for the B cations to move off center. Therefore, simple perovskites with $t > 1$ are usually ferroelectric (FE). For BZ, the sizes of the Ba and Zr ions ($R_{Ba}=1.61 \text{ \AA}$ and $R_{Zr}=0.72 \text{ \AA}$), in their O₁₂ and O₆ cage ($R_O=1.35 \text{ \AA}$) exactly balance, leading to $t=1$, so the cubic structure should have no driving force to deform to a lower symmetry. It also has a stable dielectric constant over a wide range of temperatures.²

The total dielectric constant is a sum of two contributions, related to the electronic (ϵ_∞) and ionic polarizabilities (ϵ_μ). For most perovskites, ϵ_∞ is small (≈ 5) and ϵ_μ is the dominant contribution at low frequency. Recent experimental studies of BZ at low temperature show that ϵ is 47 at 0 K and some interesting quantum effects are present, though not large in magnitude.³ Reference 3 also presents a density functional theory (DFT) study in which ϵ of BZ is 65 at 0 K, as well as a path integral quantum Monte Carlo (PIQMC) study which calculates an ϵ of 55. Both overestimate experimental results. DFT inaccuracies have been known for some time in describing ferroelectric systems.⁴ It is, however, surprising that DFT is inaccurate for a system as simple as paraelectric BZ.

Here, we show that at low temperatures, the ground state structure of BZ is not accurately represented by a five atom cell of $P_{m\bar{3}m}$ symmetry. A larger supercell with the lower $P\bar{1}$ symmetry is energetically favored. The calculated value of ϵ for this low symmetry structure is in agreement with experimental results. Most importantly, the relationship between the breaking of structural symmetry and the change in dielectric response is elucidated.

II. METHODOLOGY

In this study, two first principles codes are used. An in-house solid state DFT code used in previous studies^{5,6} and the ABINIT software package⁷ are used to relax the ionic positions and lattice constants. Local density approximation (LDA) of the exchange correlation functional and a $4 \times 4 \times 4$ Monkhorst-Pack sampling of the Brillouin zone⁸ are used for all calculations. The ground state energy is converged to within 10 meV and the lowest phonon frequency to within 4 cm^{-1} when comparing a $6 \times 6 \times 6$ and $4 \times 4 \times 4$ Monkhorst-Pack grid sampling of the five atom unit cell. All atoms are represented by norm-conserving optimized⁹ designed nonlocal¹⁰ pseudopotentials. All pseudopotentials were generated using the OPIUM code.¹¹ The calculations are performed with a plane wave cutoff of 50 Ry.

Once the structure is fully relaxed, response function^{12,13} calculations are performed with ABINIT to generate $D_{\alpha\beta}(i,j)$, the mass weighted dynamical matrix.

$$D_{\alpha\beta}(i,j) = \frac{\partial^2 E}{\sqrt{m_i m_j} \partial \tau_{i\alpha} \partial \tau_{j\beta}}. \quad (2)$$

Once normalized, each eigenvalue is ν_μ^2 , the frequency squared of a normalized eigenvector a_μ . Born effective charge tensors, $Z_{i\alpha\beta}^*$, are also calculated for each atom. Each mode μ has a mode effective charge, $Z_{\mu\alpha}^*$, defined as

$$Z_{\mu\alpha}^* = \sum_{i\beta} \frac{Z_{i\alpha\beta}^*(a_\mu)_{i\beta}}{m_i^{1/2}}, \quad (3)$$

Contributions to the dielectric response arise only from the IR active modes.¹⁴ These modes have a nonzero $Z_{\mu\alpha}^*$, and are used to calculate ϵ_μ , the contribution to the dielectric constant from mode μ ¹⁵ as

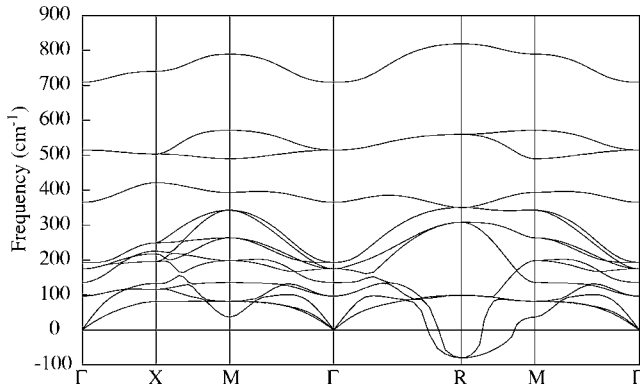


FIG. 1. The calculated phonon band structure of the five-atom high-symmetry BZ structure. Our results match well with the previously published BZ phonon band structure in Ref. 3. In particular, our unstable mode at R is -79 cm^{-1} , in close agreement with their -63 cm^{-1} .

$$\epsilon_{\mu\alpha\beta} = \frac{Z_{\mu\alpha}^* Z_{\mu\beta}^*}{4\pi^2 \epsilon_0 V v_{\mu}^2}, \quad (4)$$

where the total ionic contribution is

$$\epsilon_{\mu} = \frac{1}{3} \sum_{\alpha} \epsilon_{\mu\alpha\alpha}. \quad (5)$$

It should be noted that the quantity in Eq. (5) is the isotropic ϵ_{μ} averaged for a powder. Calculations are performed for a perfect crystal. The powder average is also obtained by taking one-third of the trace of the dielectric tensor of the perfect single crystal.

III. RESULTS AND DISCUSSION

A. Five-Atom BZ calculations

The ground state five atom BaZrO_3 is a cubic perovskite structure where all ions occupy high symmetry positions. The relaxed DFT lattice constant of this cell was $a = 4.157$ \AA , which is -0.8% less than the experimental lattice constant $a = 4.192$ \AA . This structure was used to calculate both a phonon band structure (Fig. 1) and ϵ . The structural and dielectric properties for the theoretical a are reported, but the salient features (structural instability, dielectric constant) were also calculated at the experimental a , and are similar for both lattice constants. The high-symmetry BaZrO_3 structure contains three IR active phonon modes in each direction.

The first set of phonon frequencies, occurring at 96 cm^{-1} , contribute the most to ϵ , as shown in Table I. These three modes are mainly large Ba displacements against its O_{12} cage into which some Zr displacement opposite its O_6 cage is mixed (Last mode). The ratio of Ba displacement to Zr displacement is about 9:1. However, due to the much larger Z^* of Zr (6.3 for Zr vs 2.7 for Ba) even such a small Zr off-center displacement makes a significant contribution to the effective charge of the mode. The IR active modes are sometimes discussed in terms of purely A-O or B-O displacements, but that simple cation motion is not justified when

TABLE I. Forty-atom BZ phonon data for IR active modes in the high-symmetry cubic structure. Frequencies are in cm^{-1} , mode effective charges, Z_{μ}^* , are in electrons. The contributions to the ϵ are calculated in SI units. Also reported are the motions that create the IR active mode.

ω	Z_{μ}^*	ϵ_{μ}	Motion
96	2.1	40.8	Ba-O
193	2.8	17.2	Zr-O
513	2.8	2.4	O_6

describing the lowest frequency phonon modes of BZ.

The second set of phonon frequencies occurs at 193 cm^{-1} , consisting of Zr motion (Slater mode). A small amount of Ba motion is also present, but the ratio of Zr off centering to Ba off centering in this mode is about 20:1. Combined with the smaller Z^* of Ba, this means that this mode is well characterized as pure B-O. The final set of phonons, at 513 cm^{-1} are caused by asymmetric O_6 cage motions. These contribute the least to ϵ .

To obtain ϵ , the contributions of ϵ_{μ} from Table I are added to ϵ_{∞} , which was calculated as 4.94. The total zero temperature dielectric constant for the high symmetry structure is 65. This value is almost double previous experimental investigations,² but agrees well with recent theoretical investigations.³

The disagreement between experimental and theoretical ϵ results suggests either an inaccuracy of LDA or an inaccurate representation of ground-state BaZrO_3 structure by a five-atom high-symmetry unit cell. DFT studies of PbZrO_3 correctly predicted the structure of this material,¹⁶ prior to experimental evidence that supported these findings.¹⁷ Calculations helped to resolve experimental structural discrepancies, leading to the correct structure of PbZrO_3 . In Refs. 3 and 18 the authors present a phonon band structure of BZ, which displays a soft mode at R , but none at Γ . Our phonon band structure of five atom BZ, presented in Fig. 1, confirms that there is no ferroelectric softening at Γ , but a rather large softening at R . This instability in BZ was also found by Zhong and Vanderbilt¹⁸ while studying cubic perovskites. The presence of an unstable mode indicates a driving force for symmetry breaking. To explore the effect of this, a larger BZ supercell is needed for accurate calculations.

B. Forty-Atom BZ calculations

The soft mode at R observed in the phonon band structure was induced in the high-symmetry structure, and the supercell was then relaxed. The relaxed low-symmetry triclinic structure had lattice constants $a = 8.313$ \AA , $b = 8.322$ \AA , and $c = 8.298$ \AA . Thus, the relaxed volume is only 0.10% less than the high-symmetry structure. The angles between lattice vectors are $\alpha = 89.97^\circ$, $\beta = 89.98^\circ$ and $\gamma = 90.15^\circ$. None of the cations shift from their high symmetry positions, consistent with an O_6 tilt mode where $t < 1$. This three-dimensional tilt is anisotropic and corresponds to an $a^-b^-c^-$ tilt system. This leads to the symmetry assignment $P\bar{1}$. The difference in en-

TABLE II. Forty-atom low-symmetry BZ phonon data for IR active modes with the irreducible representation A_{μ} . Frequencies are in cm^{-1} , mode effective charges, Z^* , are in e . The contributions to ϵ are calculated in SI units. For each IR active mode, the atomic motions are described.

ω	Z_{xx}^*	Z_{yy}^*	Z_{zz}^*	ϵ_{xx}	ϵ_{yy}	ϵ_{zz}	Motion
106	1.3	1.3	0.5	12.1	11.7	1.9	Ba-O
107	0.5	0.5	0.2	2.0	1.9	0.3	Ba-O
114	0.4	0.4	1.8	1.0	0.8	21.8	Ba-O
125	1.2	1.3	0.0	8.5	9.0	0.0	Ba-O
184	0.2	0.3	0.1	0.1	0.2	0.0	Zr-O
192	0.3	0.7	0.0	0.3	1.1	0.0	Zr-O
195	1.3	2.3	1.0	3.6	12.2	2.2	Zr-O
196	0.3	1.0	2.7	0.2	2.0	16.3	Zr-O
197	2.5	1.3	0.2	14.1	3.5	0.1	Zr-O
211	0.6	0.6	0.0	0.7	0.6	0.0	Zr-O
307	0.2	0.1	0.6	0.1	0.0	0.3	Ba, Zr-O
308	0.4	0.4	0.2	0.2	0.1	0.1	Ba, Zr-O
501	1.5	1.9	1.2	0.8	1.2	0.5	O_6
502	0.8	0.9	2.4	0.2	0.3	1.9	O_6
505	2.1	1.7	0.0	1.4	0.9	0.0	O_6

ergy between the high and lowered symmetry structures was 8 meV per unit cell, which is larger than the 1.5 meV difference presented in Ref. 3. Octahedral tilt angles range between 3.6 and 4.2°, in accordance with the structure presented in Ref. 3. A subsequent phonon response calculation on the tilted pseudo-cubic structure showed that no negative frequency modes were present. Unlike our calculations, low temperature x-ray diffraction and neutron scattering experiments are unable to detect this tilting in BZ.³ Current experimental evidence is unclear. The relevant x-ray reflections for oxygen-based symmetry breaking would be weak, due to the scattering factor of O. We propose the tilted structure based on quantum mechanical energy minimization and consequent dielectric response (see below) and we suggest further experimental investigation to directly confirm the predicted structure.

Analysis of the low-symmetry (Table II and Fig. 2) phonon modes show that there are more IR-active phonon modes than in the high-symmetry cell. The IR-active modes are no longer of pure x , y or z character. However, they can still be distinguished as Ba-O (Last mode), Zr-O (Slater mode), or O_6 based. Likewise, the frequency ranking of the modes is still lowest for Ba-O, higher for Zr-O, and highest for the O_6 . The Ba-O modes are clustered around 115 cm^{-1} , about 10% higher in frequency than for the high-symmetry cell. The energies of the Zr-O and the O_6 modes are essentially unchanged from their respective 5 atom cell values. Interestingly, a new band of modes is generated by this structure around 300 cm^{-1} which do not contribute as much to ϵ_{μ} as the three previously mentioned sets of modes.

Comparison of the ϵ_{μ} values in Tables I and II shows that the contribution of the mainly Ba modes to ϵ has decreased by half, whereas the contribution of the Zr modes and the O_6 modes has remained the same. The new modes around

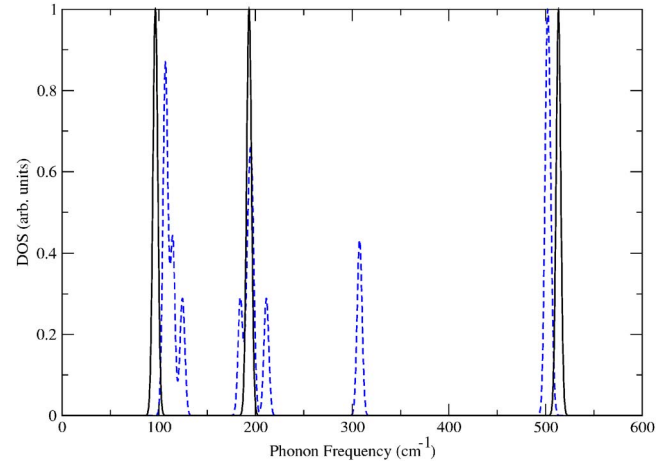


FIG. 2. (Color online) Gamma-point phonon DOS of the high-symmetry BaZrO₃ structure, solid black line, and the fully relaxed pseudo-cubic supercell, dashed line. The most important changes are the upshift in Ba-O mode frequencies (from 96 to 100–130 cm^{-1}) and the appearance of new modes around 300 cm^{-1} .

300 cm^{-1} do not contribute significantly. The total ϵ_{μ} is 45 in the x , y , and z directions, and the powder average is therefore also 45. This is in contrast with 60 calculated for the 5 atom cell. We find that ϵ_{∞} is still 4.94, and the total ϵ is 50, in agreement with low temperature experimental data.³ Thus, we find that it is necessary to include the O_6 tilt to correctly represent the dielectric response of BZ at low temperature.

We now discuss the physical reasons behind the changes in the dielectric response induced by octahedral tilting. As noted above, the weaker dielectric response of the low-symmetry BaZrO₃ structure is caused by the 40% drop in the contribution of the low frequency Last mode. To some extent, this effect can be rationalized by the rattling cation model.¹⁹ As the O_6 cages tilt, the O atoms are brought closer to the Ba atom. This reduces the volume of the Ba-O₁₂ cage leaving less room for Ba to rattle around in response to an applied electric field. More precisely, the shorter Ba-O distances lead to a stiffening of the potential energy surface felt by the Ba. This gives rise to a smaller dielectric response, as ϵ_{μ} is proportional to $1/\omega^2$. However, examination of Ba-O modes shows that ω shifts up by about 10%. This should lead to about 27% decrease in ϵ_{μ} , accounting for about half of the Ba-O mode ϵ_{μ} change. The other factor that weakens the dielectric response is the decrease in the mode effective charge Z_{μ}^* , which is significantly smaller for the low-symmetry structure than for the 5 atom high-symmetry structure. Since Eqs. (3) and (4) show that ϵ_{μ} is proportional to the square of $Z_{\mu\alpha}^*$, distribution of Z_{μ}^* over multiple modes leads to a 20% decrease in ϵ_{μ} .

Comparison of the Ba-O phonon eigenvectors for the two structures shows that induced Zr off-centering is smaller for the Last mode in the 40 atom low symmetry structure than in the 5 atom high-symmetry mode. It is this reduction in the induced Zr displacement that gives rise to the smaller Z_{μ}^* . Physically, the smaller induced Zr displacement points to a weakened coupling between Ba and Zr displacements. The coupling between Ba and Zr displacement is most likely due

to Pauli repulsion.²⁰ In the low-symmetry structure O_6 tilting as well as increased O motion in x and y directions in the Last mode eigenvector moves an O atom between Ba and Zr. This partially screens the Ba-Zr interactions, leading to a smaller Z_{μ}^* .

IV. CONCLUSIONS

We have presented calculations that reveal interesting structural and dielectric properties in the seemingly simple material $BaZrO_3$. At zero temperature, the high-symmetry model proved inadequate for calculating the dielectric constant. Large supercells were used in order to find the equilibrium structure, which exhibits octahedral tilts. These tilts have a significant effect on the low frequency Ba-O Last mode and its contribution to the dielectric constant. Allowing octahedral tilts in the first principles modeling of $BaZrO_3$ resolves the discrepancy between recent theoretical and experimental investigations of low temperature dielectric constant. The boundary of stability of octahedral rotations occurs at $t=1$, but that is based purely on ionic size. Ba is relatively polarizable and wants shorter bonds to O than pre-

dicted by standard size arguments due to covalency. It effectively acts like a smaller ion, permitting octahedral rotations, and BZ behaves like $t < 1$. Yet BZ remains a PE material, and not AFE as $PbZrO_3$. The decrease in t leads to dramatic changes in how the material responds as a dielectric, due to changes in mode frequencies and effective charges. Moreover, the understanding of how octahedral tilting can change dielectric response should give insight into alloying strategies for future dielectric materials design.

ACKNOWLEDGMENTS

This work was supported by the Office of Naval Research under Grant No. N-00014-00-1-0372, and through the Center for Piezoelectrics by Design under Grant No. N00014-01-1-0365, GAANN support from the US Department of Education and the University of Pennsylvania, and the National Science Foundation under both the IMI Program Award No. DMR 0409848 and the MRSEC Program NSF DMR00-29909. We also acknowledge the support of the DoD HPCMO, DURIP and NSF CRIF program, Grant No. CHE-0131132.

¹W. Fortin, G. E. Kugel, J. Grigas, and A. Kania, *J. Appl. Phys.* **79**, 4273 (1996).

²I. Levin, T. G. Amos, S. M. Bell, L. Farber, T. A. Vanderah, R. S. Roth, and B. H. Toby, *J. Solid State Chem.* **175**, 170 (2003).

³A. R. Akbarzadeh, I. Kornev, C. Malibert, L. Bellaiche, and J. M. Kiat, *Phys. Rev. B* **72**, 205104 (2005).

⁴R. E. Cohen, *J. Phys. Chem. Solids* **57**, 1393 (1996).

⁵I. Grinberg and A. M. Rappe, *AIP Conf. Proc.* **677**, p. 130 (2003), ISSN: 0094-243X, URL: <http://dx.doi.org/10.1063/1.1609946>.

⁶S. E. Mason, I. Grinberg, and A. M. Rappe, *Phys. Rev. B* **69**, 161401(R) (2004).

⁷X. Gonze, J.-M. Beuken, R. Caracas, F. Detraux, M. Fuchs, G.-M. Rignanese, L. Sindic, M. Verstraete, G. Zerah, F. Jollet *et al.*, *Comput. Mater. Sci.* **25**, 478 (2002).

⁸H. J. Monkhorst and J. D. Pack, *Phys. Rev. B* **13**, 5188 (1976).

⁹A. M. Rappe, K. M. Rabe, E. Kaxiras, and J. D. Joannopoulos,

Phys. Rev. B **41**, 1227 (1990).

¹⁰N. J. Ramer and A. M. Rappe, *Phys. Rev. B* **59**, 12471 (1999).

¹¹<http://opium.sourceforge.net>.

¹²X. Gonze and C. Lee, *Phys. Rev. B* **55**, 10355 (1997).

¹³P. Ghosez, J.-P. Michenaud, and X. Gonze, *Phys. Rev. B* **58**, 6224 (1998).

¹⁴E. Cockayne and B. P. Burton, *Phys. Rev. B* **62**, 3735 (2000).

¹⁵E. Cockayne, *J. Eur. Ceram. Soc.* **23**, 2375 (2003).

¹⁶D. J. Singh, *Phys. Rev. B* **52**, 12559 (1995).

¹⁷S. Teslic and T. Egami, *Acta Crystallogr., Sect. B: Struct. Sci.* **B54**, 750 (1998).

¹⁸W. Zhong and D. Vanderbilt, *Phys. Rev. Lett.* **74**, 2587 (1995).

¹⁹H. D. Megaw, *Acta Crystallogr., Sect. B: Struct. Crystallogr. Cryst. Chem.* **B24**, 149 (1968).

²⁰I. Grinberg, V. R. Cooper, and A. M. Rappe, *Nature (London)* **419**, 909 (2002).